

Article

Numerical Analysis of Bearing Capacity in Deep Excavation Support Structures: A Comparative Study of Nailing Systems and Helical Anchors

Seyyed Alireza Taghavi ^{1,2}, Farhad Mahmoudi Jalali ³, Reza Moezzi ⁴ , Reza Yeganeh Khaksar ^{1,*}, Stanisław Waclawek ⁵ , Mohammad Gheibi ⁵  and Andres Annuk ^{4,*} 

¹ Department of Civil Engineering, Sadjad University of Technology, Mashhad 9188148848, Iran; seyed@tultech.eu

² Association of Talent under Liberty in Technology (TULTECH), 10615 Tallinn, Estonia

³ Department of Civil Engineering, Faculty of Engineering, Islamic Azad University, Tabriz Branch 5157944533, Iran; farhadmahmoudijalali@gmail.com

⁴ Institute of Forestry and Engineering, Estonian University of Life Science, Kreutzwaldi 56/1, 51014 Tartu, Estonia; reza.moezzi@emu.ee

⁵ Institute for Nanomaterials, Advanced Technologies and Innovation, Technical University of Liberec, Studentská 1402/2, 461 17 Liberec, Czech Republic; stanislaw.waclawek@tul.cz (S.W.); mohammad.gheibi@tul.cz (M.G.)

* Correspondence: rezayeganeh@sadjad.ac.ir (R.Y.K.); andres.annuk@emu.ee (A.A.)

Abstract: The increasing demand for deep excavations in construction projects emphasizes the necessity of robust support structures to ensure safety and stability. Support structures are critical in stabilizing excavation pits, with a primary focus on enhancing their bearing capacity. This paper employs finite element modeling techniques to conduct a numerical analysis of nails and helical anchors' bearing capacity. To reinforce the stability of pit walls, selecting an appropriate method for guard structure construction is imperative. The chosen method should efficiently redistribute forces induced by soil mass weight, displacements, and potential loads in the pit vicinity to the ground. Various techniques, including trusses, piles, cross-bracing systems, nailing, and anchorage systems, are utilized for this purpose. The study evaluates numerical models for two guard structure configurations: nailing systems and helical anchorage. It examines the impact of parameters such as displacement, helical helix count, helix diameter variations, and the integration of nailing systems with helices. Comparative analyses are conducted, including displacement comparisons between different nailing systems and helical anchor systems, along with laboratory-sampled data. The research yields significant insights, with a notable finding highlighting the superior performance of helical bracings compared to nailing systems. The conclusions drawn from this study provide specific outcomes that contribute valuable knowledge to the field of deep excavation support structures, guiding future design and implementation practices.

Keywords: geotechnical simulation; Abaqus software; helical anchors; soil stability; nailing analysis; soil displacement assessment



Citation: Taghavi, S.A.; Jalali, F.M.; Moezzi, R.; Khaksar, R.Y.; Waclawek, S.; Gheibi, M.; Annuk, A. Numerical Analysis of Bearing Capacity in Deep Excavation Support Structures: A Comparative Study of Nailing Systems and Helical Anchors. *Eng* **2024**, *5*, 657–676. <https://doi.org/10.3390/eng5020037>

Academic Editor: Antonio Gil Bravo

Received: 26 February 2024

Revised: 6 April 2024

Accepted: 10 April 2024

Published: 18 April 2024



Copyright: © 2024 by the authors. Licensee MDPI, Basel, Switzerland. This article is an open access article distributed under the terms and conditions of the Creative Commons Attribution (CC BY) license (<https://creativecommons.org/licenses/by/4.0/>).

1. Introduction

With the growth of population and urbanization, the optimal use of land has become a crucial issue. The construction of residential, administrative, and commercial complexes in urban areas, especially in large cities, highlights the importance of detailed field and geotechnical studies to ensure the proper design and stability of the guard structures [1]. The stability of excavations and the bearing capacity of foundations are critical factors [2–4], and the method of pit excavation and stabilization of open pits are key considerations for successful construction projects [5].

Excavations at great depths require careful consideration of effective land use, time constraints, and the stability of pit walls, which some experimental studies have conducted recently [6,7]. In order to minimize the disturbance to the surrounding area and prevent potential collapse, guard structures are implemented before foundation construction to increase the strength of the excavated walls. Various methods can be used for restraining and building a guard structure, but nailing or anchoring is one of the most effective and commonly used methods [8,9]. With the unpredictable behavior of soil and the presence of adjacent buildings and facilities, it is necessary to take action to ensure the stability of the excavation site and protect against potential risks [10].

Soil nail walls are constructed by erecting a front face support and inserting closely spaced steel bars or sections in the existing ground to provide passive reinforcement. Various parameters are influential on the stability of the nailed wall, such as nail spacing, whose effect on the global stability of soil-nailed walls has been well studied [11]. Anchoring, on the other hand, is a more complex and specialized method of providing stability to structures. Anchors come in a variety of types, including helical anchors, driven piles, and drilled shafts, and are designed to provide support in a variety of soil and geologic conditions. Anchors are commonly used in foundation work, including building foundations, retaining walls, and bridges, where they are used to transfer the load of the structure to the ground [12]. The problems of designing a well and implementing guard structures in the field of civil engineering vary widely, and therefore there is a need to review and study geotechnical data, available materials, implementation methods, financial costs, and project construction time. To select the stabilization system of the pit walls using guard structures, factors such as excavation depth, soil type, existing overhead, boundary conditions, materials, and equipment are influential. The following are a few current, pertinent studies: In a superdeep excavation in Beijing, Wang et al. [13] studied the stress and deformation properties of a composite soil-nailed wall and an anchored soldier pile wall combined retaining system. Their study shed light on the variables influencing the performance of the retaining structure and emphasized the need to limit lateral displacement during excavation. Similar to this, during the construction of a deep foundation pit, Sun et al. [14] examined the behavior of a three-pile and two-anchor rod support system in an anhydrous sand pebble strata. Their investigation clarified the axial force distribution along anchor rods and the passive force-bearing property of soil-nailed walls, which advances our knowledge of the behavior of support systems in a range of scenarios. Mun et al. [15] employed a hybrid soldier pile, tieback, and soil-nailed shoring wall to reduce shoring wall displacement in crowded metropolitan locations. Their results illustrated the usefulness of using thorough numerical simulations in shoring system design by proving how well this hybrid technique reduced wall displacement below allowable bounds. In order to enlarge a hillside roadway, Zhou et al. [16] devised a laterally cantilevered space frame system that uses ground tieback anchors as essential structural elements. They successfully redistributed surcharge loadings on slopes, which provided advantages over traditional approaches in terms of lower construction costs and environmental impact. Additionally, in soft soil places close to the sea, Junding Liu et al. [17] looked into the deformation management of deep foundation pit excavation. Using both numerical modeling and long-term in situ monitoring, their study examined the deformation characteristics of a geometrically difficult deep foundation hole project in Taizhou. Future projects with comparable conditions might refer to the study's insightful findings on the deformation features of deep foundation pit excavation in soft soil areas.

A prestressed anchor holding system with a bearing structure under the anchor head was presented by Jia et al. [18] as an alternative to rigid retaining techniques in deep foundation pits. Their study proved how well the technology controlled deformation and reduced environmental impact, providing useful solutions for excavation operations in metropolitan areas. Furthermore, in large-scale deep foundation pit situations, Liu et al. [19] examined the "corner effect" in the optimum design of soil-nailed wall-retaining pile-anchor cable supporting systems. Their work underlined the need to take lateral forces

into account in support structure design by proposing an optimization technique to lower construction costs while meeting safety criteria. A case study of a deep excavation next to a residential structure in Tehran using high-pressure grouted soil nails and anchors for lateral support was given by Mirlatifi [20]. His research validated the efficacy of the chosen design techniques by demonstrating the relationship between numerical forecasts and observed displacements and reinforcing pressures. In order to conduct a deep foundation excavation in a second-tier inland city, Chen et al. [21] examined several retaining system designs, highlighting the significance of striking a balance between structural capabilities and cost-effectiveness. Their results highlighted the advantages of hybrid methods in lowering displacements and improving safety during excavation, such as soil-nailed walls in conjunction with pile anchors. Nisha et al. [22] examined the difficulties in urban design and construction while presenting a case study of deep excavation for an office building in Bengaluru. Their research made clear how crucial numerical modeling is to the efficient design of shoring systems and the prompt implementation of corrective actions to reduce the risk to nearby structures. In their investigation of several stabilizing techniques for deep excavation pit walls in Ardabil, Zolfegharifar et al. [23] emphasized the need to establish a stable and safe environment prior to excavation. In order to evaluate the stability of excavation walls, their study used finite element and limit equilibrium analysis, which gave important insights into geological and geotechnical issues. In addition to the above studies, Table 1 also summarizes an approach-based literature review that aims to explore the current state of research on the topic of the bearing capacity of nails and helical anchors in order to provide a more comprehensive overview of the existing literature and identify gaps in the research that need to be addressed.

Table 1. The literature review of the bearing capacity of nails and helical anchors.

Method	Approach	Reference
Numerical analysis	The paper presents the design process for the micropiles, including the determination of the load capacity and the spacing and depth of the micropiles.	[24]
Laboratory tests	The authors conducted a series of laboratory tests to investigate the effects of various factors, such as pile diameter, helix spacing, and soil density, on the bearing capacity of helical piles.	[25]
Laboratory tests	The paper gives details about the testing program and the results of the tests, which showed that the CPT or CPTu methods can be used to accurately predict the bearing capacity of helical piles.	[26]
Finite element analysis	The authors used finite element analysis to study how a retaining wall with helical anchors behaved when the anchors were set up in different ways.	[27]
Numerical modelling	The paper presents a case study on the performance of a helical soil-nailed wall used to support a bridge abutment.	[9]
Finite element analysis	The study showed that the pull-out capacity of the helical multiple anchors increased with an increase in the number of helices and the embedment depth of the anchors.	[28]
Finite element analysis	This study investigates the ideal ratio of S/D_h , which represents the spacing between helical plates and the diameter of the helical plate, for multiple helical piles.	[29]

Table 1 shows that most of the previous studies that looked at the effect of different factors on the bearing capacity of nails and helical anchors used numerical and finite element modeling. As mentioned in Table 1, several researchers have pointed out the effects of spacing between helical plates on bearing capacity, but extensive and practical research has not been conducted in this case.

This novel study examines the comparison of the final bearing capacity of nails and helical anchors in a very detailed and rigorous way to address a gap in the field. We aim to use Abaqus v. 6.12 [30] software to examine an excavated model with helical anchors to calculate their maximum capacity when expanded in the specified soil. A method for accurately assessing soil behavior is simulation, which provides insightful information for

improving and stabilizing soil [31–35]. At first, numerical modeling is used to verify the validity of the topic discussed in the selected basic article, and then by making changes in the implementation of helical anchors, such as changing the diameter of helixes, combining simple anchors with helixes, increasing the number of helixes, and a gradual increase in the load, the change in the head of the wall reaches the allowed value of the regulation. In this research, an attempt has been made to discuss and investigate the impact of excavation behaviors and the values obtained from the displacement and deformation of the pit wall, which are modeled by the various implementations of helical and simple anchors in Abaqus.

2. Material and Methods

2.1. Model Planning

Before carrying out any excavation operation, geotechnical studies and research should be conducted to determine the soil type of the site. In this research, the existing dug wells, water aqueducts from the past to the present, and underground facilities should also be examined. The underground water level is another issue that should be paid special attention to. If there is a heavy load, especially dynamic and seismic loads such as pools around the drilling site, the necessary measures must be included in the process requirements to reduce these loads.

One of the most significant, and perhaps one of the most crucial, influencing factors in geotechnical studies is the soil behavior model. The results and analysis design may be significantly impacted by the selection of appropriate soil behavior models. In the research that has been conducted, an effort has been made to look into the behavior of the drilling process and the values of displacements and deformations of the pit wall. These values are first verified by numerical modeling with a laboratory model, and then the drilled model with a nailing system and helical bracing system is analyzed using the Abaqus software. The models created by the software are introduced in Table 2. Figure 1 shows the descriptive diagram parameters used in Table 2.

Table 2. Specifications of models introduced in Abaqus software.

Model Number	Helix Diameter (mm)	Type of Bracing System	The Number of Helixes
1	-	Nailing	-
2	15	Helical anchor	3
3	15	Helical anchor	4
4	40	Helical anchor	3
5	40	Helical anchor	4
6	45	A combination of helixes and nailing	3
7	45	Helical anchor	3

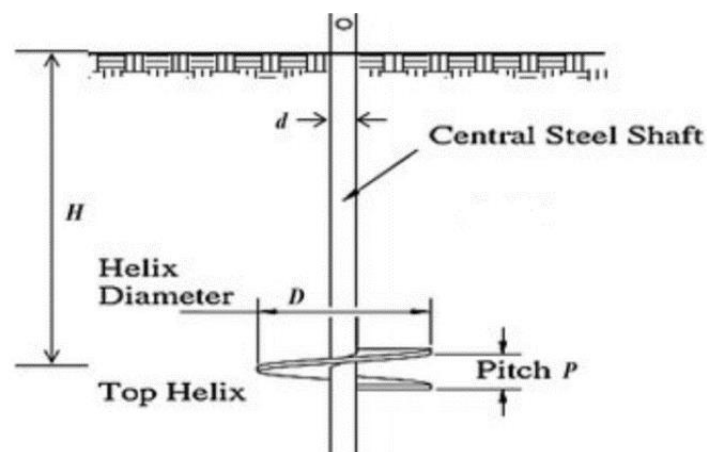


Figure 1. Details of helical anchor.

In contrast to other models, model 7 gradually applies a load to the model until the top of the wall changes to the permitted value of the regulation. This results in a different amount of load on the soil than other models.

2.2. Material Specifications

It should be noted that the main scales are not always practical and applicable due to constraints, which will be discussed further. Two Helical anchor and nailing systems are taken into consideration in this modeling and analysis under entirely identical conditions. In the Abaqus modeling, the excavation wall height is 80 cm, whereas in the actual excavation operation, the walls are 8 m high. After the excavation operation is complete, a top wall made of mesh network and shotcrete concrete is used in the two implementation methods of nailing and helical anchor systems. These walls typically range in thickness from 5 to 10 cm in reality, though this can vary depending on the soil type and other project-specific factors. A 5 cm thick concrete wall has been selected for the design and modeling of the final procedure. Materials that can provide the compressive and tensile strengths of shotcrete concrete as well as the tensile strength of the mesh network used in the excavated wall should be used for the design of the wall. In order to provide this feature, polymer derivatives were used. A compressed Teflon sheet that is fireproof (PTF) and has a compressive strength and high hardness of approximately 1 GPa is used in the numerical modeling.

Based on calculations in Appendix A, it was determined that a 5 cm concrete wall in the real model is equivalent to a Teflon wall with a thickness of 1.5 cm in the software model for designing the wall thickness in numerical modeling with a laboratory scale of 1:10. Steel plates of a certain weight were used for loading in both models. In terms of soil moisture percentage, it was determined that the value during the experiments was equal to 10%. In modeling, the soil density was also set to 70% based on the characteristics of the soil, which will be covered in more detail. And in the designs, the heel of the wall was taken into account as the heel of the stuck wall. In the real model, holes with a diameter of 10 to 25 cm are used for the drilling design of the nailing system. For this model, holes with a 10 cm diameter served as the basis, and they were scaled down to a 1 cm diameter in a 1:10 ratio. The used strands' diameter can range from 15 to 40 mm, and they can be made of a variety of materials and alloys. The strands used in the software modeling had a 15 mm diameter, which was converted to 1.5 mm by applying the modeling scale. In the real model, the nails are spaced apart by 150 to 300 cm and 100 to 250 cm, respectively. For the purposes of this simulation, the horizontal and vertical distances between the holes were set, as depicted in Figure 2a.

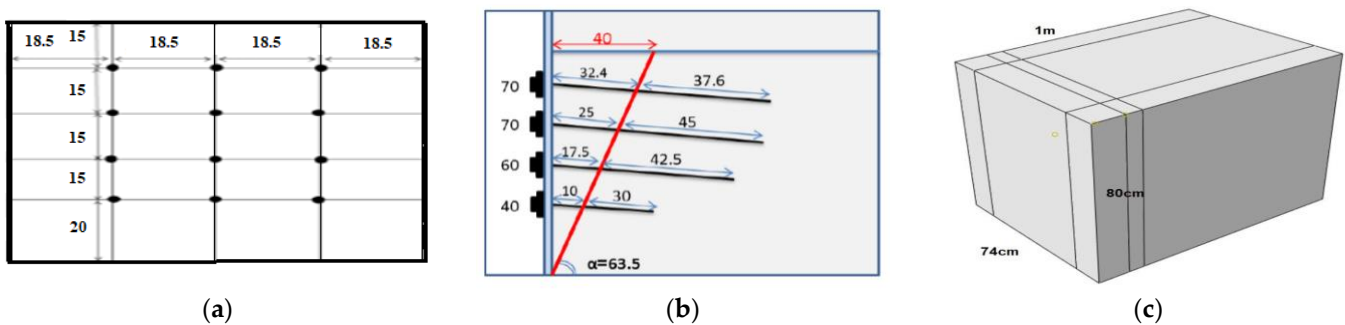


Figure 2. General configuration in this study. (a) The distance between the holes; (b) simulated model geometry; (c) soil geometry in modelling.

We determined the nail length based on the required carrying capacity and the technical characteristics of the soil. Most of these designs shared similar implementation strategies and guiding principles. The regulations for the size and length of the bars in Figure 2b suggested the following models. Figure 2c also displays the spatial shape of the simulation element.

The diameter of the helix can range from 15 to 45 cm in accordance with American regulations and taking into account the circumstances and characteristics of the soil. So, using a scale of 1:10, 4.5 cm plates were used in this simulation.

The use of square and solid rods would improve the tensile performance of bracings, but since these materials were not available for this modeling, solid circular rods were chosen instead. Typically, square and curved sections of rods with diameters ranging from 1.5 to 4 cm are used. Iron wire with a 1.5 mm diameter was used in this simulation, scale-adjusted. Additionally, it is advised that the distance between two helical anchors be 2.5 to 3.5 times the diameter of helices in relation to each other in order to comply with the current regulations regarding the distance of the helices from one another. As a result, in the simulation, the ratio of the distance between the helix was taken to be roughly three times the helix’s diameter in length.

The helical bracing, the soil, and the guard structure make up the model’s three main components. In the experiment, three different types of helices with lengths of 40, 60, and 70 cm were used. The rows were positioned in the soil at an angle of 10 degrees, with the bottom row being 40 cm long, the second row being 60 cm long, and the top two rows being 70 cm long. The soil in this model had the following measurements: 100 × 80 × 74 cm. Its geometry is shown in Figure 2c, and Table 3 lists the material properties of the soil.

Table 3. Soil characteristics.

Stickiness	Internal Friction Angle (Degrees)	Dry Density (kg/m ³)	Minimum Dry Density (kg/m ³)	Maximum Dry Density (kg/m ³)	Sand
0.05	37	1546.03	1392	1644	Chiruk WT60 (Regional)

The main rod’s diameter was 1.5 mm, its plates’ diameter was 4.5 cm, and their thickness is 1.5 mm. Three times the plates’ diameter, or 13.5 cm, separates them from one another. It has three dimensions, each 40, 60, and 70 cm in length. In Figure 3, all three models are displayed.

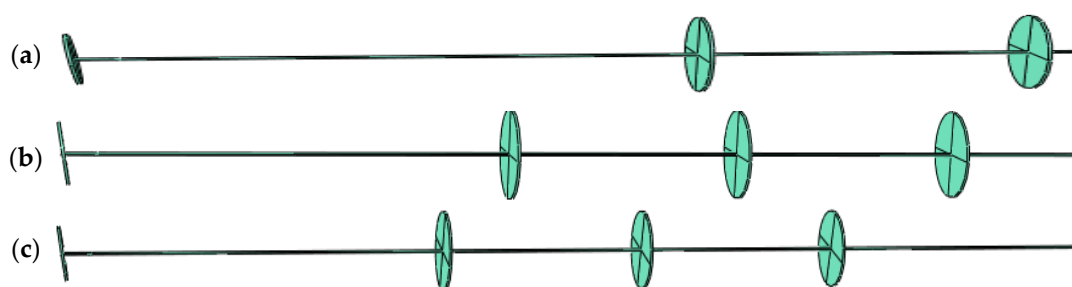


Figure 3. (a) Helical anchor with dimensions of 40 cm; (b) helical anchor with dimensions of 60 cm; (c) helical anchor with dimensions of 70 cm.

2.3. Loading, Boundary Conditions, and Meshing

As can be seen, the horizontal distance between the helices is 18.5 cm, and the vertical distance between them is 15 cm. The assembly model for this layout in Abaqus software is also presented in Figure 4a.

Given that the soil is modeled as a solid, Figure 4b should be followed when placing the helical bracings in the ground and arming them. The next step is to ascertain the friction coefficient and contact properties on all surfaces after all helical bracings have been defined. Typically, 0.3 is thought to be the approximate value of the coefficient of friction between soil and other components. By choosing the General Contact type after calculating the friction coefficient, it is possible that the software will take into account contact wherever it exists in the models. The model’s loading and boundary conditions are established in

this section. The lower portion of the soil is completely bound, as shown in Figure 4c, in accordance with the type of model.

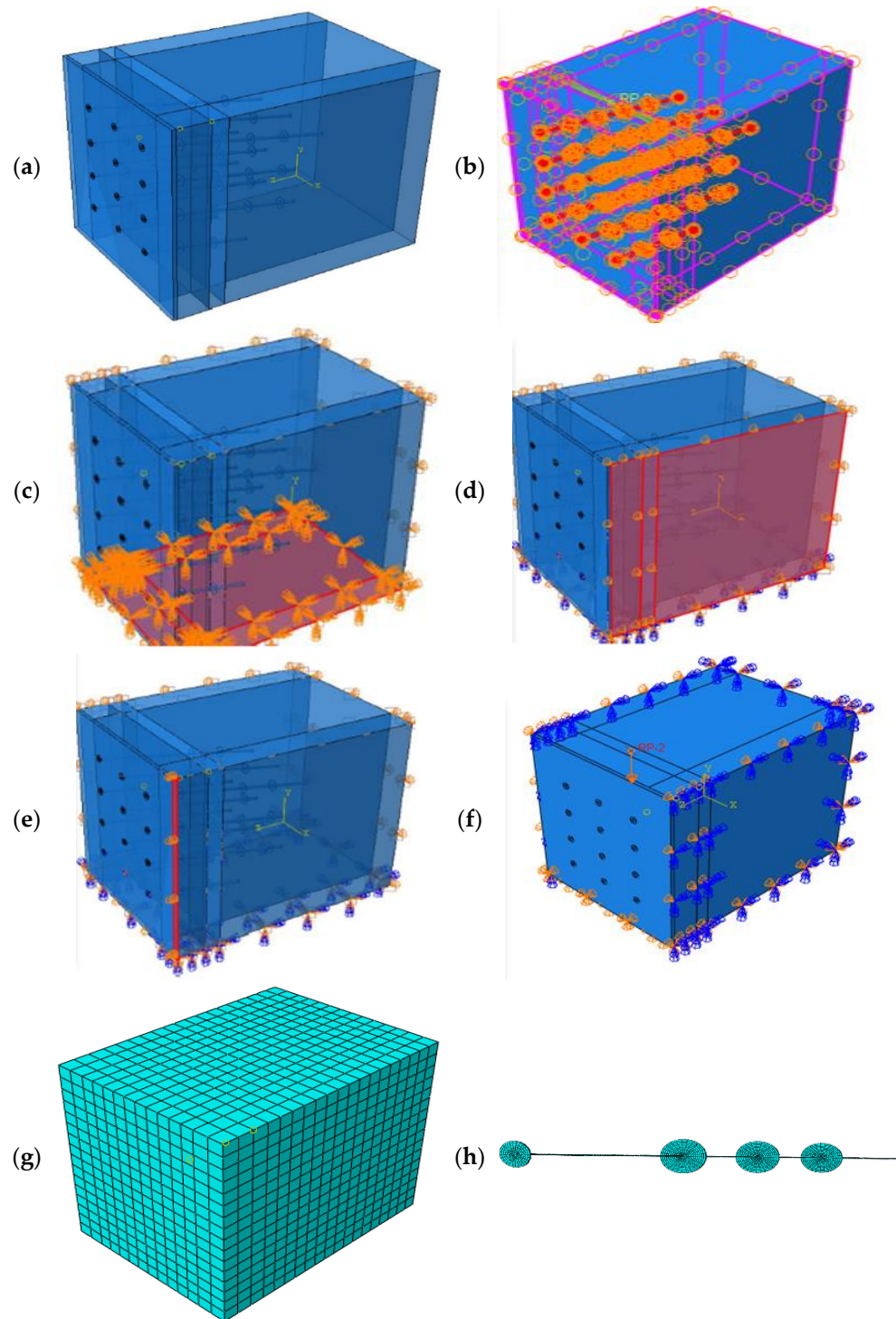


Figure 4. (a) Assembly model with helical anchor; (b) defining the model for burying the anchor in the soil; (c) complete binding of the lower part of the soil; (d) binding of the right wall in the structure; (e) binding the guard wall; (f) applying load on the upper part of the soil; (g) soil model meshing; (h) helical anchor meshing.

The upper surface of the soil is the only surface that is bounded and Figure 4d depicts one of these walls. The upper and lower sides of the guard wall are tied vertically; the other degrees of freedom are left free. Figure 4e represents how one of the surfaces has

been bound. The final step involves applying the incoming load, whose maximum weight is 288 kg, to the soil as a point load at the location depicted in Figure 4f. The model's meshing section is then shown. Figure 4g displays the mesh model for the soil, which has a granularity of 0.01 m (10 mm). Figure 4h shows the meshing model of one of the helical anchors, which was produced using 0.0079 m as the mesh size. Finally, the meshing of the guard wall is appropriately considered.

3. Numerical Model

Validation of the Base Numerical Model

In this section, the results of the numerical model for verification are compared with the results of the base physical model.

The calibration test specifications depicted in Figure 5b encompass a thorough experimental setup designed to refine the model's accuracy. It is imperative to note that the dataset employed for this calibration is sourced from an authentic project carried out in Mashhad City, Iran. Notably, the calibration process uniquely incorporates a specific segment of the project data within the ambit of the current research undertaking.

During the experimental phase, a scaling factor of 1:10 is applied, aligning the scale of the experiment with that of the simulation for accurate comparison. As delineated in Figure 5b, the experimental setup adopts a backfill approach, distinct from real-world activities where soil immersion via screwing is commonplace. Consequently, the phenomenon of soil loosening, inherent to screwing methods, is absent in the laboratory analysis and results. Consequently, in the simulation procedure, the effect of soil loosening is omitted, mirroring the conditions of the experimental setup. This meticulous alignment ensures that the simulation faithfully reflects the experimental conditions, enhancing the reliability and applicability of the model's outcomes.

The comparison of the change in horizontal locations obtained by the numerical model and the physical model based on Figure 5a shows that the displacement along the wall in the two models has a slight difference, which indicates the acceptable performance of the numerical model (Table 4). Comparing the change in horizontal locations obtained by numerical models and physical models is a crucial aspect of validating numerical simulations in various fields, including engineering and fluid dynamics. It helps assess the accuracy and reliability of numerical models in representing real-world phenomena. Our findings are distinct because, in some cases, earlier studies have not been able to compare the horizontal displacement along the wall from both numerical and physical results. For example, the study by Misir discusses the numerical model calibration of U-shaped multi-leaf stone masonry wall specimens tested under ambient vibrations. While the exact details of the results are not provided In the search results, It can be Inferred that the comparison of numerical and physical models was conducted to assess the performance of the numerical model in predicting horizontal displacements along the wall [36]. Another study by J García-Alba evaluates numerical models' performance in describing flows of positively buoyant jets. While it does not directly mention the comparison of horizontal displacements, it indicates the use of numerical models to simulate physical phenomena [37]. In a study by MA Bouarroudj, the differences between numerical and experimental results in single-strut models are discussed. This could potentially include the comparison of horizontal displacements, although specific details are not provided [38].

Table 4. Comparison of displacement of two models (physical and numerical).

Difference Percentage of Experimental and Numerical Model	Difference between Experimental and Numerical Model (cm)	Displacement Rate in the Numerical Model (cm)	Displacement Rate in the Physical Model (cm)
2%	0.1	4.7	4.8

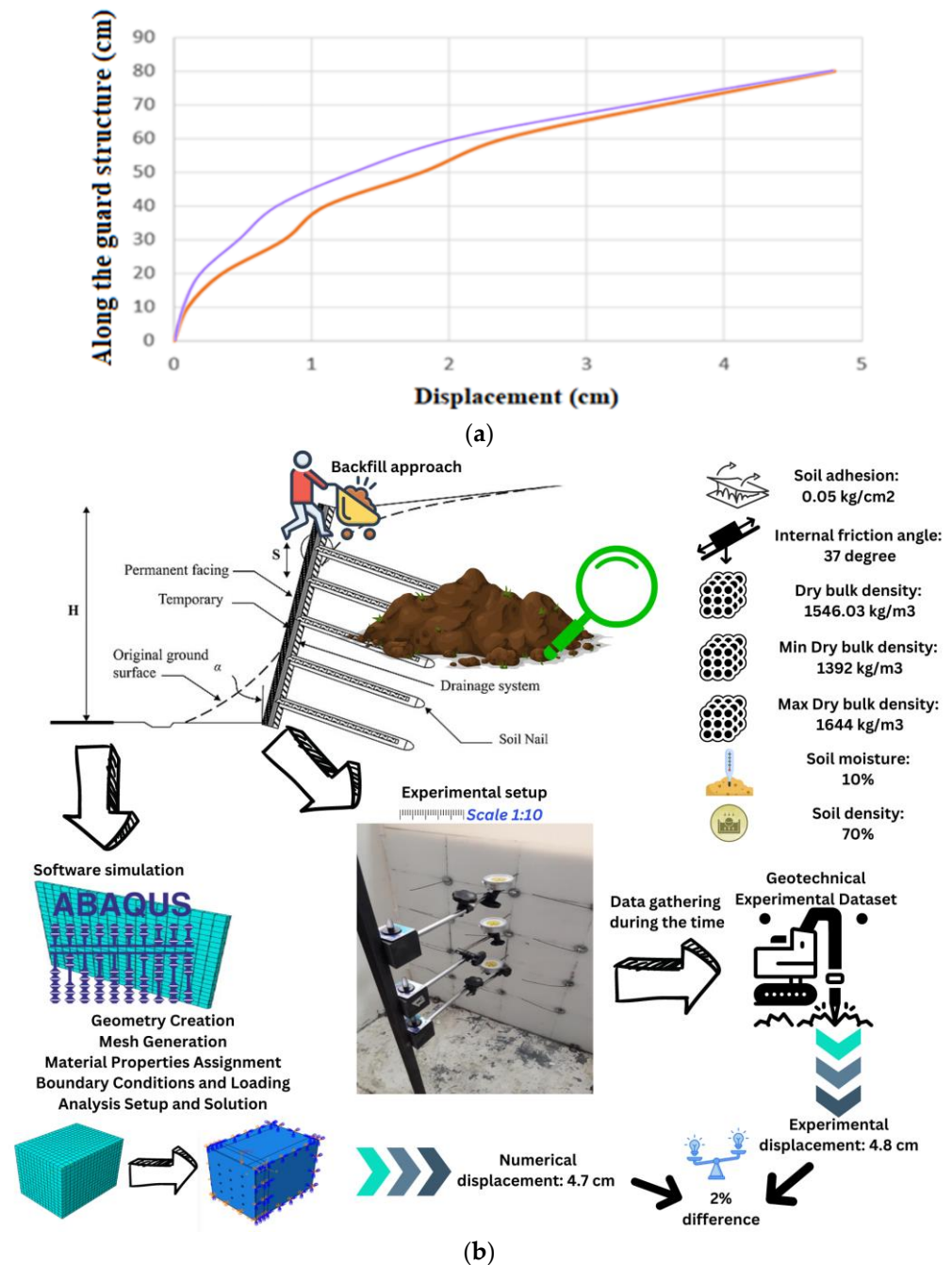


Figure 5. The descriptions of (a) displacement along the wall from the Abaqus model in orange; displacement along the wall from the base in the physical model in purple; and (b) experimental setup specifications.

4. Results and Discussion

In this section of the research, the results extracted from the modelling are presented. In the modelling performed by the Abaqus software, the changes and displacement of the pit wall are studied during the use of nailing and helical bracing. The helical model is divided into six different models, including changes in the number of helices, the diameter of the helices, and the gradual addition of load until reaching the permitted position change of the regulation. In this research, two basic models, including nailing and helical bracing, are used to stabilize the pit wall.

The results are analyzed in seven models; the main characteristics of each model are described below:

1. Nailing with a diameter of 45 mm and 3 helixes;
2. Helical anchor with a diameter of 15 mm and 3 helixes;
3. Helical anchor with a diameter of 15 mm and 4 helixes;
4. Helical anchor with a diameter of 40 mm and 3 helixes;
5. Helical anchor with a diameter of 40 mm and 4 helixes;
6. The combination of helical and nailing with a diameter of 45 mm and 3 helixes with an arrangement of one in between;
7. Helical bracing as a gradual increase in load permitted by the regulations with a diameter of 45 mm and 3 helixes.

Each model is modelled while taking into account the parameters, and the results are then saved in an Excel file. As a result, at the conclusion of the work, the effects of the change in the shape of the pit wall, capacity, and incoming energy have been compared.

4.1. Type of Bracing

To study the impact of different bracing systems on embankment stability, models 1 (nailing system), 7 (bracing helical anchor system), and 6 (combined nailing and helical bracing system) are being compared in Figure 6.

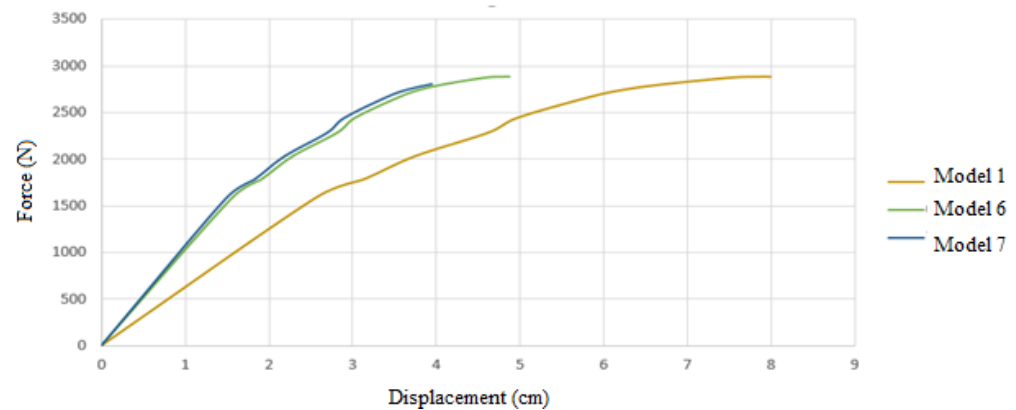


Figure 6. Comparison of three models based on bearing force.

In Figure 6, the displacement of the applied force for each of the models can be seen until the end of the analysis.

With a digging height of 80 cm and a horizontal displacement of the wall equal to 0.002 times that height, the allowable displacement is determined to be 0.16 cm. In order to establish the bearing capacity of the models according to the permissible displacement authorized by laws, it is essential to identify the force value that causes this displacement in the models, as seen in Figure 7.

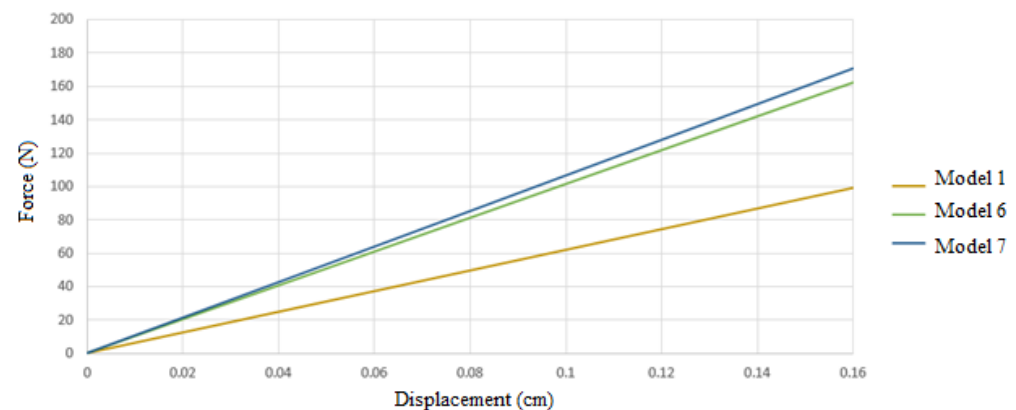


Figure 7. Comparison of the model's displacement depending on the standard's allowable limit.

Figure 8 displays the wall displacement for each model. Model number 7 (3 to 35 mm helixes) experiences the least amount of wall displacement.

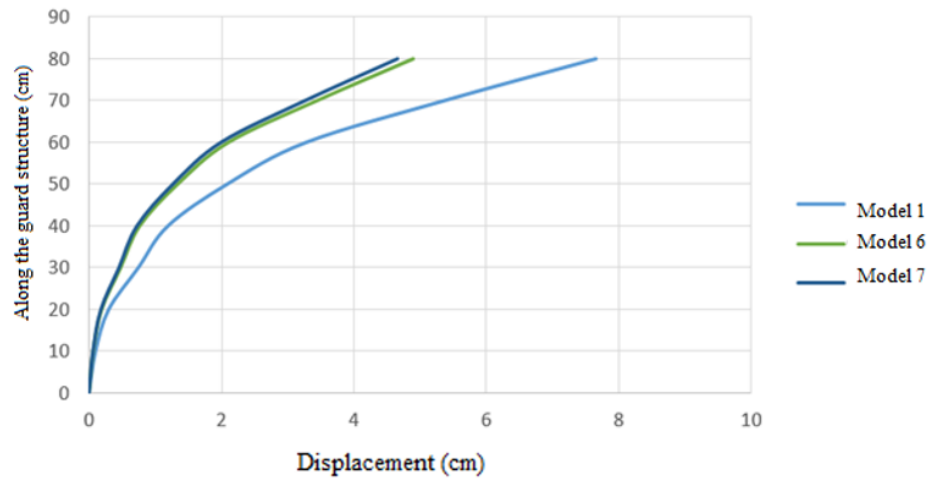


Figure 8. Comparing displacement along the guard structure.

Figure 9 displays the energy input for each model taken from the software, indicating that model number one necessitates the most energy input.

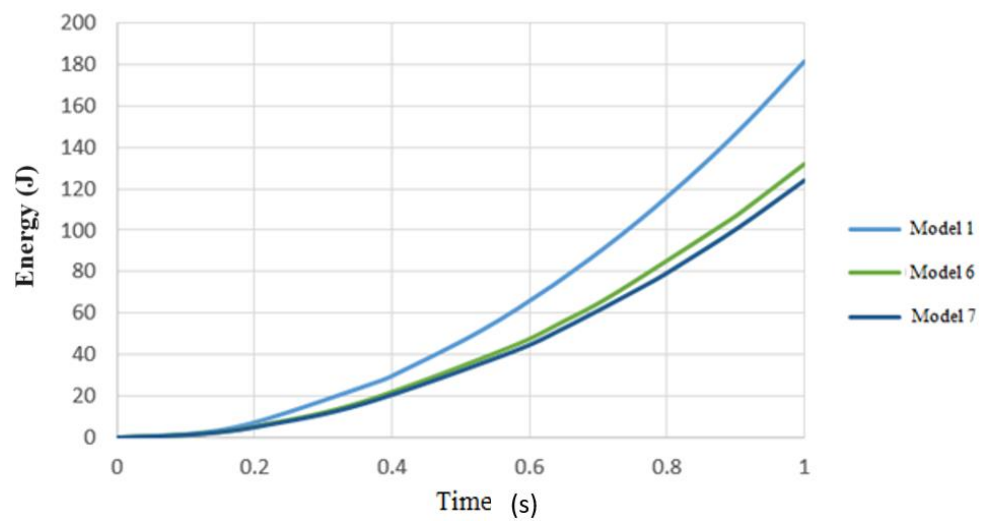


Figure 9. Comparing the energy input required by various models.

Table 5 displays the maximum energy input, displacements, and bearing capacity for each model. The final conclusion will be drawn based on these statistics.

Table 5. Results obtained from the analysis of models.

The Maximum Energy Input to the Model (J)	Maximum Displacement of the Model (cm)	The Capacity of the Model Is Based on the Amount of Displacement Allowed by the Regulations (N)	Model Number
181	7.66	100	1
132	4.88	162	6
124	4.66	170	7

4.2. The Diameter of the Helixes

In order to check the effect of the diameter of the helix used in the helical bracing system, model number 2, which has a diameter of 15 mm, and model number 4, which has

a diameter of 40 mm, and model number 7, which has a diameter of 45 mm, were compared with each other.

In Figure 10, the displacement of the applied force for each of the models can be seen until the end of the analysis.

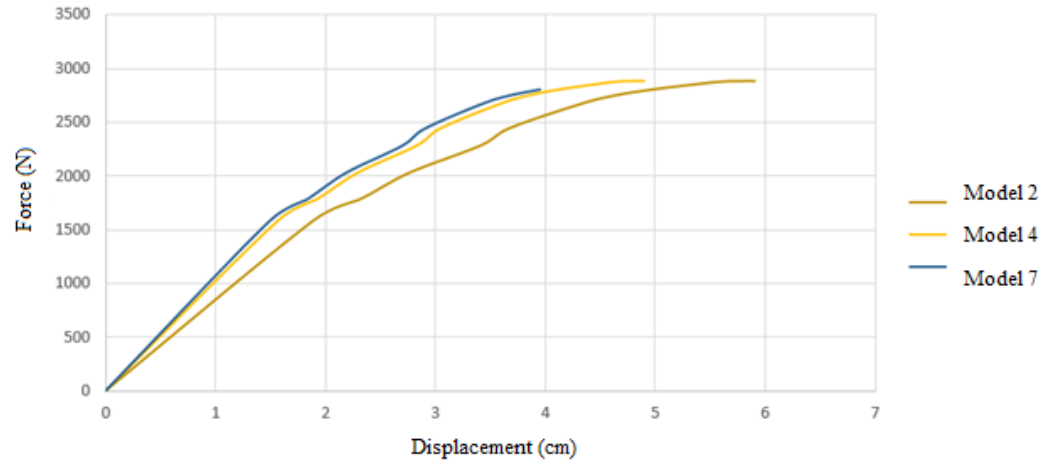


Figure 10. Comparison of three models based on bearing force.

Considering that the amount of horizontal displacement of the wall is equal to 0.002 of the digging height and that the digging height is 80 cm, the allowed displacement is calculated as 0.16 cm. Therefore, by obtaining the amount of force that causes this displacement in the models according to Figure 11, it is possible to calculate the bearing capacity of the models based on the permissible displacement of the regulations.

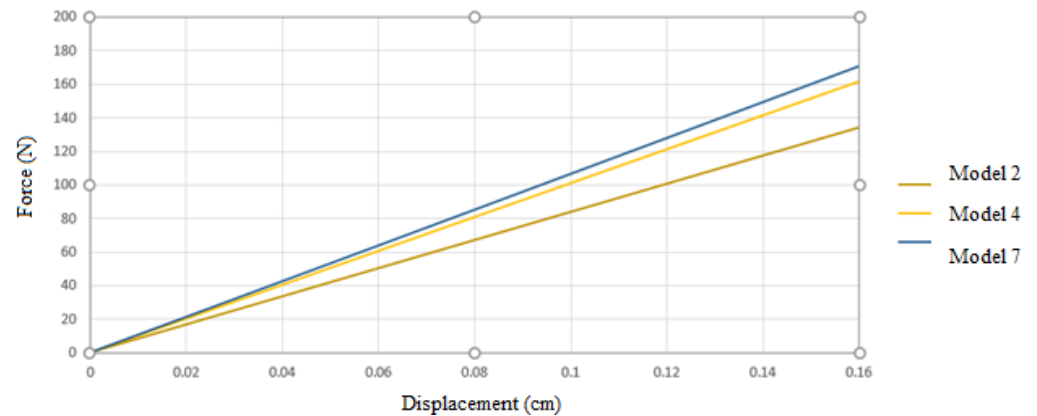


Figure 11. Comparison of the model’s displacement depending on the standard’s allowable limit.

In Figure 12, the displacement along the wall is shown for each of the models; according to the diagram, the lowest amount of wall displacement occurred in model number 7 (3 to 45 mm helixes).

In Figure 13, the energy input to each of the models extracted from the software can be seen.

Table 6 provides data on the maximum energy input, displacements, and bearing capacity of each model, which will be used to draw the ultimate conclusion in the summary.

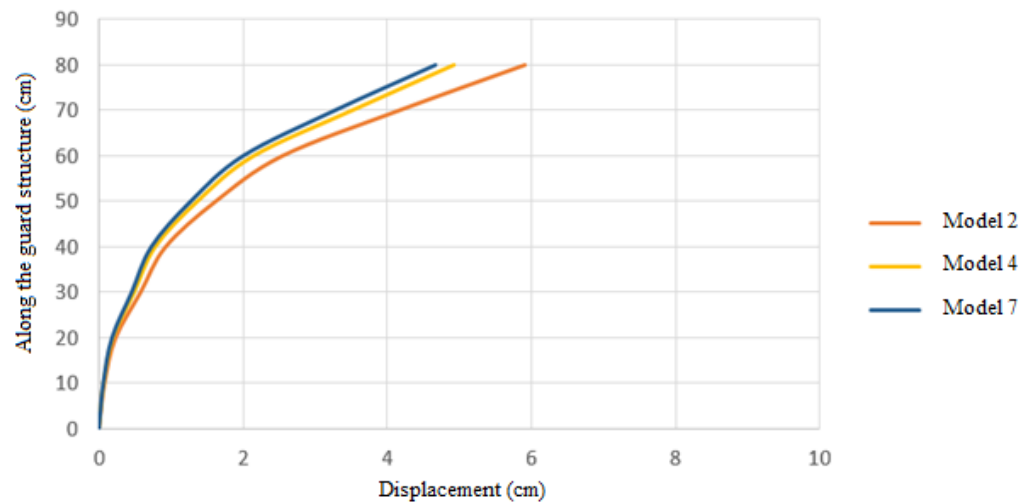


Figure 12. Comparing displacement along the guard structure.

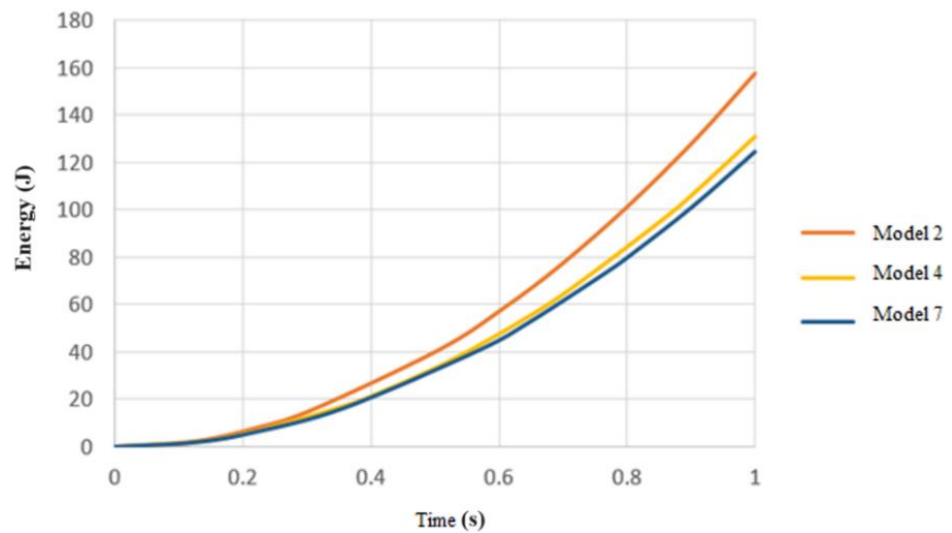


Figure 13. Comparing the energy input required by various models.

Table 6. Results obtained from the analysis of models.

The Maximum Energy Input to the Model (J)	Maximum Displacement of the Model (cm)	The Capacity of the Model Is Based on the Displacement Allowed by the Regulations (N)	Model Number
158	5.9	130	2
131	4.9	164	4
124	4.66	170	7

4.3. The Number of Helixes

In order to check the effect of the number of helix plates used in the helical bracing system, considering the constant consideration of the plate diameter, once for the plate diameter of 15 mm, model number 2, which has 3 helix plates, and model number 3, which has 4 helix plates, are compared with each other. Again, for the 40 mm plate diameter, model No. 4, which has 3 helixes, and model No. 5, which has 4 helixes, are compared.

4.3.1. Helixes with Diameter of 15 mm

For the case with helixes of 15 mm diameter, the results are as below.

In Figure 14, the displacement of the applied force for each of the models can be seen until the end of the analysis.

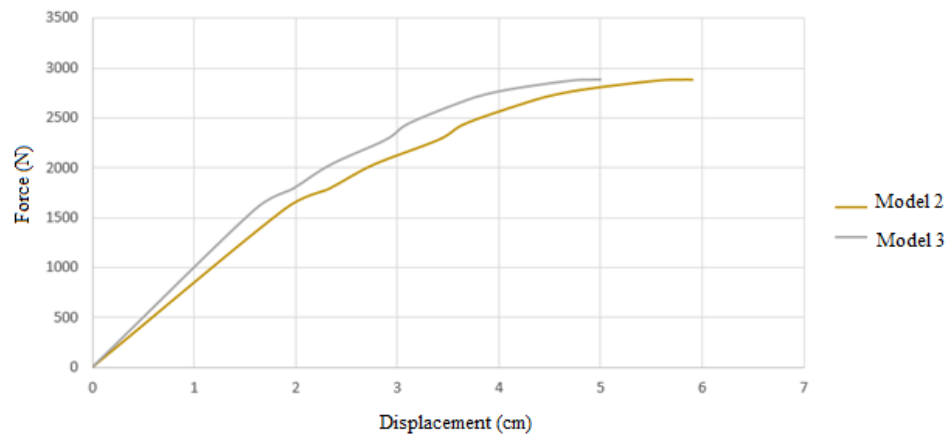


Figure 14. Comparison of two models based on bearing force.

Considering that the amount of horizontal displacement of the wall is equal to 0.002 of the digging height and that the digging height is 80 cm, the allowed displacement is calculated as 0.16 cm, according to Figure 15. Therefore, by obtaining the amount of force that causes this displacement in the models, it is possible to calculate the bearing capacity of the models based on the permissible displacement of the regulations.

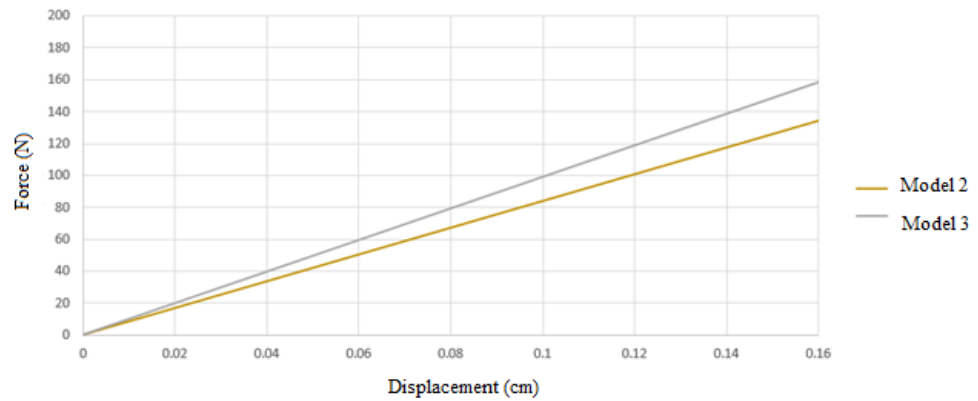


Figure 15. Comparison of the model's displacement depending on the standard's allowable limit.

In Figure 16, the displacement along the wall is shown for each of the models. According to the diagram, the lowest amount of wall displacement occurred in model number 3 (4 to 15 mm helixes).

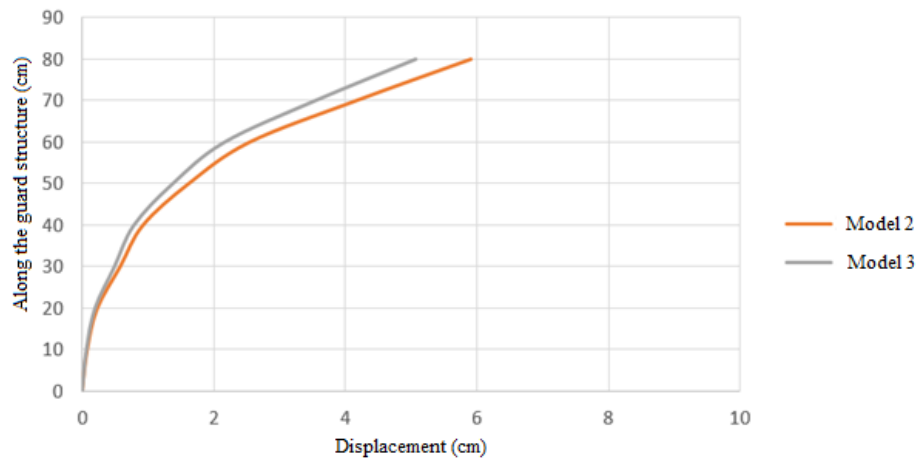


Figure 16. Comparing displacement along the guard structure.

In Figure 17, the amount of energy input to each of the models extracted from the software can be seen.

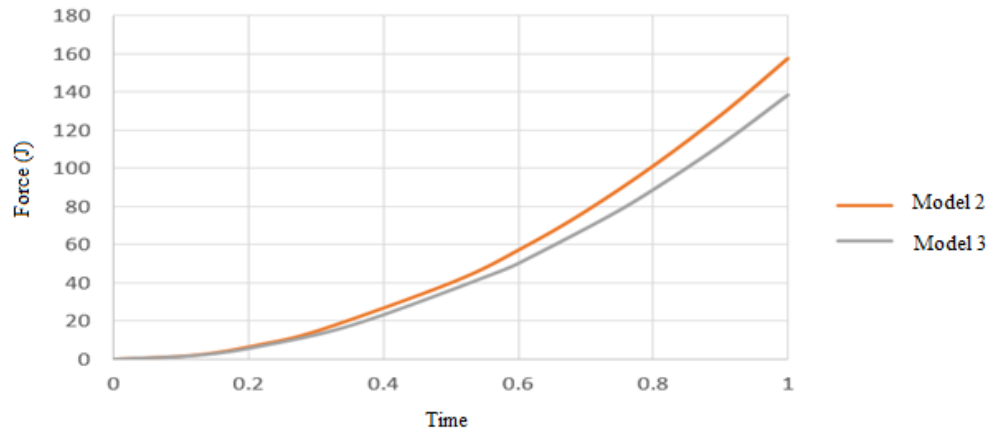


Figure 17. Comparing the energy input required by various models.

In Table 7, the maximum amount of energy entered into the structure, the displacements, and the bearing capacity of each model are presented, and in the summary of the results, the ultimate conclusion will be derived from these data.

Table 7. The results obtained from the analysis of the models.

The Maximum Energy Input to the Model (J)	Maximum Displacement of the Model (cm)	The Capacity of the Model Is Based on the Displacement Allowed by the Regulations (N)	Model Number
158	5.9	130	2
138	5	159	3

4.3.2. Helixes with a Diameter of 40 mm

In Figure 18, the displacement of the applied force for each of the models can be seen until the end of the analysis.

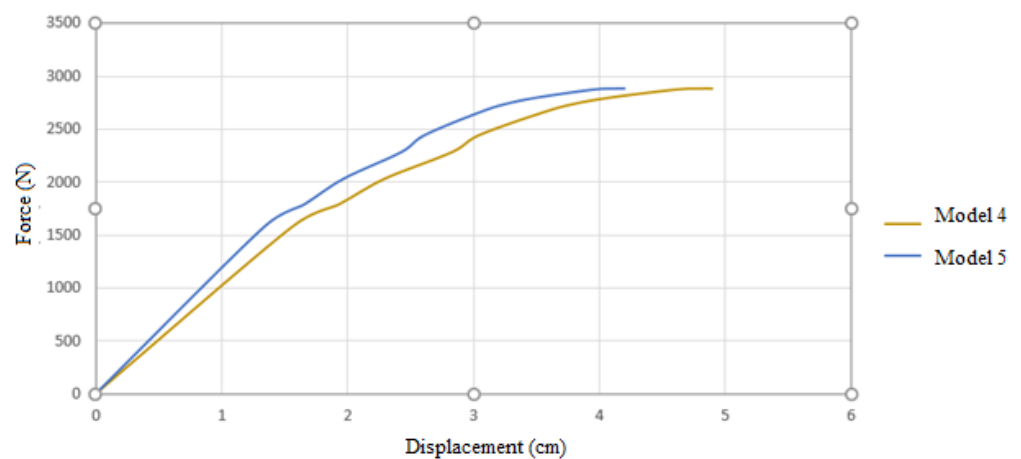


Figure 18. Comparison of two models based on bearing force.

The permitted displacement is computed as 0.16 cm, taking into account that the wall’s horizontal displacement is equal to 0.002 of the digging height and that the digging height is 80 cm (according to Figure 19). Therefore, based on the permitted displacement of the regulations, it is possible to compute the bearing capacity of the models by obtaining the amount of force that generates this displacement in the models.

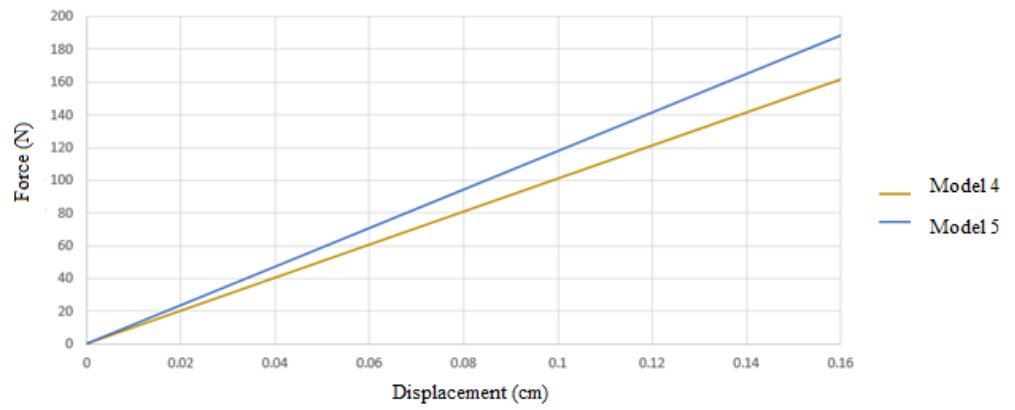


Figure 19. Comparison of the model’s displacement depending on the standard’s allowable limit.

In Figure 20, the displacement along the wall is shown for each of the models. According to the diagram, the lowest amount of wall displacement occurred in model number 5 (4 to 40 mm helixes).

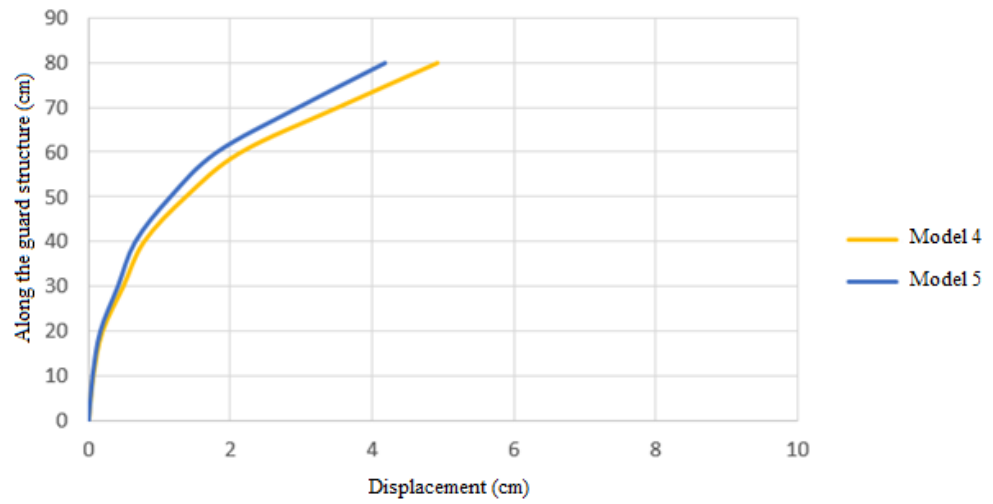


Figure 20. Comparing displacement along the guard structure.

In Figure 21, the amount of energy input to each of the models extracted from the software can be seen.

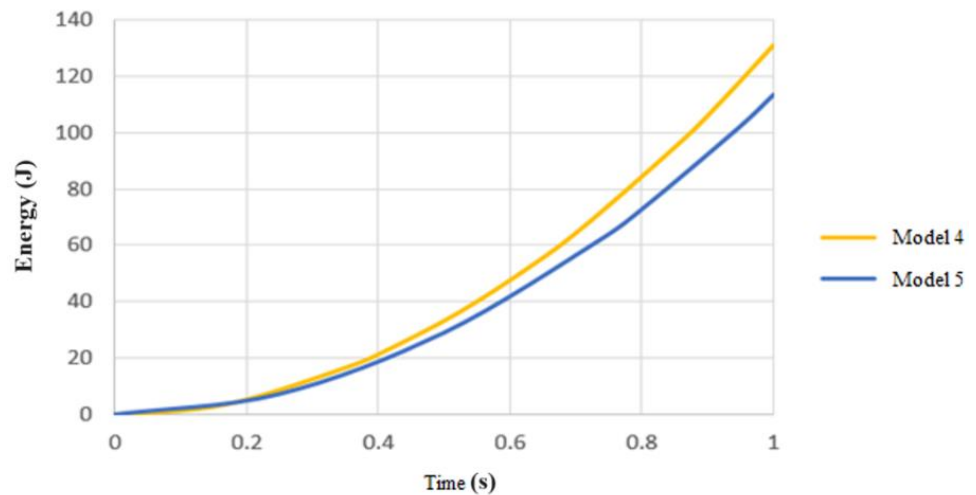


Figure 21. Comparing the energy input required by various models.

The maximum energy entered into the structure, the displacements, and the load capacity of each model are listed in Table 8, and the conclusions that follow will be based on these data and the findings summary.

Table 8. The results obtained from the analysis of the models.

The Maximum Energy Input to the Model (J)	Maximum Displacement of the Model (cm)	The Capacity of the Model Is Based on the Displacement Allowed by the Regulations (N)	Model Number
131	4.9	164	4
113	4.2	190	5

The existing model has been carried out in order to obtain a numerical analysis of the bearing capacity of helical and nailing through finite element modeling. In this way, the conclusion of the research is of great importance because it can be a foundation for solving the problems or improving the current situation and pave the way to a more optimized solution. Based on the available results, we can observe the effect of parameters such as the type of bracing system, the diameter, and the number of helices. Based on this, in order to check the type of bracing system, models 1, 6, and 7 were used, and for the helical anchor system, compared to the nailing system, the bearing capacity, wall displacement, and energy input to the structure increased by 41%, 39%, and 31%, respectively.

For the helical and nailing combined restraining and bracing system, compared to the nailing system, the amount of capacity, wall displacement, and energy input to the structure increased by 38%, 36%, and 17%, respectively. Now, according to the comparisons made regarding the type of bracing system, the bracing helical anchor system performed better than other systems and improved the performance and capacity of the model.

In order to check the diameter of the helices, model numbers 2, 4, and 7 were used, and according to the comparisons made, the helical anchor with a plate diameter of 45 mm performed better than other systems and improved the performance and capacity of the model. By changing the diameter of the plate from 40 to 45 mm, the capacity of the structure increased by 3.5%, and also, by changing the diameter from 15 to 45 mm, the bearing capacity of the structure increased by 23%.

The effect of the number of helices on the structural responses was investigated in two cases; the first case was for a helical anchor with a helix diameter of 15 mm and 3 and 4 helices. And the second model was the helical anchor with a helix diameter of 40 mm and 3 and 4 helices. In both cases, increasing the number of helices improved the performance and capacity of the model. In the first case, the increase in the bearing capacity was 18%, and in the second case, it was 13%.

The study's results reveal the performance and effectiveness of two distinct deep excavation support systems: the nailing system and the helical anchor system. The behavioral variations across these systems offer vital insights into their structural features and operational mechanisms. The nailing system's brittle and fragile behavior, along with its rapid upward deformations as it reaches the breaking point, emphasize the significance of comprehending the impact of injected concrete on its load-bearing capability. This trend indicates that the effectiveness of the nailing method could be affected by factors like the quality of concrete injection and soil adhesion. In contrast, the helical anchor system operates more softly, displaying steady upward deformations until breaking. The flexibility of steel helices in the helical anchor system contributes to its overall performance against overhead loads, making it a promising option for deep excavation support. The comparative analysis reveals that the helical anchor system, particularly configurations with multiple helices of larger diameters, outperforms the nailing system in terms of displacement and energy input. This underscores the importance of considering the design parameters and configurations when selecting the most suitable support system for a given excavation project.

5. Conclusions

- The analysis results indicate distinct behavioral differences between the nailing system and the helical anchor system.
- The nailing system exhibits brittle, fragile behavior with rapid upward deformations upon reaching the breaking threshold, likely attributed to the contribution of injected concrete to its bearing capacity.
- In contrast, the helical anchor system operates more softly, showing steady upward deformations until breaking, with steel helixes contributing to its flexibility and overall performance against overhead loads.
- Based on the available results, the capacity of load-bearing, displacement, and energy input in the bracing system with four plates of 40 mm compared to the nailing system changed, with a 47% increase, 45% decrease, and 37% decrease, respectively. These values indicate the highest level of performance of the bracing systems compared to the nailing system.
- The capacity of the construction is increased by 3.5 percent by increasing the diameter of the plate from 40 to 45 mm. Additionally, the structure's capacity increases by 23% when the diameter is changed from 15 to 45 mm.
- Based on the conducted investigations, the best-performing bracing system configurations are ranked as follows:
 1. Anchor with 4 helixes of 40 mm diameter.
 2. Anchor with 3 helixes of 45 mm diameter.
 3. Combined mode of helical anchor and nailing.
 4. Anchor with 3 helixes of 40 mm diameter.
 5. Anchor with 4 helixes of 15 mm diameter.
 6. Anchor with 3 helixes of 15 mm diameter.
- The conclusions drawn from this research suggest several areas for further investigation, including consideration of soil saturation, comparison of outcomes using another software such as Analysis System (ANSYS), and variations in soil properties.

Author Contributions: Conceptualization, S.A.T. and R.Y.K.; methodology, M.G. and S.W.; software, F.M.J. and R.M.; writing—original draft preparation, validation, R.M. and A.A.; formal analysis, M.G. and S.W.; review and editing; S.A.T., F.M.J. and M.G., writing—review and editing, R.M. and A.A.; visualization, M.G.; supervision, R.Y.K. and A.A. All authors have read and agreed to the published version of the manuscript.

Funding: This research did not receive any funding.

Institutional Review Board Statement: Not applicable.

Informed Consent Statement: Not applicable.

Data Availability Statement: The data that support the findings of this study are available upon reasonable request from the corresponding author.

Conflicts of Interest: The authors declare no conflicts of interest.

Appendix A

$$E_p = 1 \text{ GPa}; E_c = 25 \text{ GPa}$$

$$N = \frac{1}{10} \rightarrow I = \left[\frac{1}{10^4} \right] \rightarrow 10^4 = \frac{E_c \frac{b h^3}{12}}{E_p \frac{b h^3}{12}} \rightarrow \frac{b = 740 * h = 5}{b = 74 * h = ?}$$

$$h^3 = \frac{25 \times 10 \times 5^3}{10^3} = 3.15 \rightarrow h = 1.46 \cong 1.5 \text{ cm}$$

References

1. Satyanaga, A.; Aventian, G.D.; Makenova, Y.; Zhakiyeva, A.; Kamaliyeva, Z.; Moon, S.-W.; Kim, J. Building Information Modelling for Application in Geotechnical Engineering. *Infrastructures* **2023**, *8*, 103. [\[CrossRef\]](#)
2. Chaabani, W.; Remadna, M.S.; Abu-Farsakh, M. Numerical Modeling of the Ultimate Bearing Capacity of Strip Footings on Reinforced Sand Layer Overlying Clay with Voids. *Infrastructures* **2023**, *8*, 3. [\[CrossRef\]](#)
3. Gokceoglu, C.; Aygar, E.B.; Nefeslioglu, H.A.; Karahan, S.; Gullu, S. A Geotechnical Perspective on a Complex Geological Environment in a High-Speed Railway Tunnel Excavation (A Case Study from Türkiye). *Infrastructures* **2022**, *7*, 155. [\[CrossRef\]](#)
4. Islam, M.N. Small Scale Experiments to Assess the Bearing Capacity of Footings on the Sloped Surface. *Eng* **2020**, *1*, 240–248. [\[CrossRef\]](#)
5. De Bruyn, I.; Prado, D.; Mylvaganam, J.; Walker, D. Geotechnical Considerations for the Stability of Open Pit Excavations at Mine Closure, Some Scenarios. In Proceedings of the 13th International Conference on Mine Closure, Perth, Australia, 3–5 September 2019; pp. 235–248. [\[CrossRef\]](#)
6. Tian, Y.; Motalleb Qaytmas, A.; Lu, D.; Du, X. Stress Path of the Surrounding Soil during Tunnel Excavation: An Experimental Study. *Transp. Geotech.* **2023**, *38*, 100917. [\[CrossRef\]](#)
7. Zhao, Y.; Chen, X.; Hu, B.; Huang, L.; Li, W.; Fan, J. Evolution of Tunnel Uplift and Deformation Induced by an Upper and Collinear Excavation: A Case Study from Shenzhen Metro. *Transp. Geotech.* **2023**, *39*, 100953. [\[CrossRef\]](#)
8. Cheng, S.-H.; Chen, S.-S.; Yang, K.-H. Self-Inspection System for Ground Anchors Monitoring on Long-Term Load Change. *Transp. Geotech.* **2022**, *36*, 100825. [\[CrossRef\]](#)
9. Yadegari, S.; Yazdandoust, M.; Momenyan, M. Performance of Helical Soil-Nailed Walls under Bridge Abutment. *Transp. Geotech.* **2023**, *38*, 100788. [\[CrossRef\]](#)
10. Koerner, R.M. In-Situ Stabilization of Soil Slopes Using Nailed or Anchored Geosynthetics. *Int. J. Geosynth. Ground Eng.* **2015**, *1*, 2. [\[CrossRef\]](#)
11. Villalobos, S.A.; Villalobos, F.A. Effect of Nail Spacing on the Global Stability of Soil Nailed Walls Using Limit Equilibrium and Finite Element Methods. *Transp. Geotech.* **2021**, *26*, 100454. [\[CrossRef\]](#)
12. Juran, I.; Elias, V. Ground Anchors and Soil Nails in Retaining Structures. In *Foundation Engineering Handbook*; Fang, H.-Y., Ed.; Springer: Boston, MA, USA, 1991; pp. 868–905, ISBN 9781461367529.
13. Wang, S.; Li, Q.; Dong, J.; Wang, J.; Wang, M. Comparative Investigation on Deformation Monitoring and Numerical Simulation of the Deepest Excavation in Beijing. *Bull. Eng. Geol. Environ.* **2021**, *80*, 1233–1247. [\[CrossRef\]](#)
14. Sun, Y.; Li, Z. Analysis of Deep Foundation Pit Pile-Anchor Supporting System Based on FLAC3D. *Geofluids* **2022**, *2022*, 1699292. [\[CrossRef\]](#)
15. Mun, B.; Oh, J. Hybrid Soil Nail, Tieback, and Soldier Pile Wall—Case History and Numerical Simulation. *Int. J. Geotech. Eng.* **2017**, *11*, 1–9. [\[CrossRef\]](#)
16. Zhou, Z.; Li, F.; Qujue, A. Laterally Cantilevered Space Frame for the Roadway Widening in Steep-Sloped Mountainous Areas. *Struct. Eng. Int.* **2008**, *18*, 254–258. [\[CrossRef\]](#)
17. Liu, J.; Ye, J.; Shen, X.; Yu, J.; Wu, T.; Yuan, J.; Ye, Q.; Wang, S.; He, H. In-Situ Monitoring and Numerical Analysis of Deformation in Deep Foundation Pit Support: A Case Study in Taizhou. *Appl. Sci.* **2023**, *13*, 6288. [\[CrossRef\]](#)
18. Jia, J.; Gao, R.; Tu, B.; Zhou, C. Application of Flexible Retaining with Prestressed Anchor to Reduce the Effect That Excavations Have on Urban Environment. *Ekoloji Derg.* **2018**, *2018*, 1833–1840.
19. Liu, L.; Wu, R.; Congress, S.S.C.; Du, Q.; Cai, G.; Li, Z. Design Optimization of the Soil Nail Wall-Retaining Pile-Anchor Cable Supporting System in a Large-Scale Deep Foundation Pit. *Acta Geotech.* **2021**, *16*, 2251–2274. [\[CrossRef\]](#)
20. Mirlatifi, S. Performance Evaluation of a 21m Deep Excavation Stabilised by Combined Soil Nails and Anchors—A Case Study. *Aust. Geomech. J.* **2013**, *48*, 203–209.
21. Chen, A.; Wang, Q.; Chen, Z.; Chen, J.; Chen, Z.; Yang, J. Investigating Pile Anchor Support System for Deep Foundation Pit in a Congested Area of Changchun. *Bull. Eng. Geol. Environ.* **2021**, *80*, 1125–1136. [\[CrossRef\]](#)
22. Nisha, J.J.; Muttharam, M.; Vinoth, M.; Prasad, C.R.E. Design, Construction and Uncertainties of a Deep Excavation Adjacent to the High-Rise Building. *Indian Geotech. J.* **2019**, *49*, 580–594. [\[CrossRef\]](#)
23. Zolfegharifar, S.Y.; Kuchesfahani, A. Geotechnical study and analysis of the stability of pit walls. *Fen Bilim. Derg. (CFD)* **2015**, *36*, 1285–1297.
24. Babu, G.L.S.; Murthy, B.S.; Murthy, D.S.N.; Nataraj, M.S. Bearing Capacity Improvement Using Micropiles: A Case Study. In Proceedings of the GeoSupport 2004; American Society of Civil Engineers: Orlando, FL, USA, 2004; pp. 692–699.
25. Abd El-Rahim, H.H.A.; Taha, Y.K.; Mohamed, W.E.D.E.S. The compression and uplift bearing capacities of helical piles in cohesionless soil. *JES J. Eng. Sci.* **2013**, *41*, 2055–2064. [\[CrossRef\]](#)
26. Fateh, A.M.A.; Eslami, A.; Fahimifar, A. Direct CPT and CPTu Methods for Determining Bearing Capacity of Helical Piles. *Mar. Georesour. Geotechnol.* **2017**, *35*, 193–207. [\[CrossRef\]](#)
27. Mahmoudi-Mehrzi, M.-E.; Ghanbari, A.; Sabermahani, M. The Study of Configuration Effect of Helical Anchor Group on Retaining Wall Displacement. *Geomech. Geoenjin.* **2022**, *17*, 598–612. [\[CrossRef\]](#)
28. Abdoli, M.; Mehrnahad, H.; Hazeghian, M. Numerical Study of Pullout Capacity of Helical Multiple Anchors for Supporting Excavations. *Road* **2023**, *31*, 279–290.

29. Vijayakumar, S.; Muttharam, M. Numerical Study on Uplift Capacity of Helical Pile Embedded in Homogeneous and Layered Soil. In *Proceedings of the Soil Dynamics, Earthquake and Computational Geotechnical Engineering*; Muthukkumaran, K., Ayothiraman, R., Kolathayar, S., Eds.; Springer Nature: Singapore, 2023; pp. 97–108.
30. *ABAQUS, Analysis User's Manual*; Version 6.12; Dassault Systemes Simulia, Inc.: Johnston, RI, USA, 2012.
31. Bozkurt, S.; Abed, A.; Karstunen, M. Finite Element Analysis for a Deep Excavation in Soft Clay Supported by Lime-Cement Columns. *Comput. Geotech.* **2023**, *162*, 105687. [[CrossRef](#)]
32. Giner, E.; Sukumar, N.; Tarancón, J.E.; Fuenmayor, F.J. An Abaqus Implementation of the Extended Finite Element Method. *Eng. Fract. Mech.* **2009**, *76*, 347–368. [[CrossRef](#)]
33. Siemens, G.A.; Bathurst, R.J.; Miyata, Y. Numerical Simulation and Parametric Analysis of Multi-Anchor Walls Using the Finite Element Method. *Transp. Geotech.* **2018**, *15*, 57–69. [[CrossRef](#)]
34. Zhuang, Y.; Wang, K. Finite Element Analysis on the Dynamic Behavior of Soil Arching Effect in Piled Embankment. *Transp. Geotech.* **2018**, *14*, 8–21. [[CrossRef](#)]
35. Al Hasani, S.; Nasrellah, H.A.; Abdulraeg, A.A. Numerical Study of Reinforced Concrete Beam by Using ABAQUS Software. *Int. J. Innov. Technol. Interdiscip. Sci.* **2021**, *4*, 733–741. [[CrossRef](#)]
36. Misir, I.S.; Yucel, G. Numerical Model Calibration and a Parametric Study Based on the Out-Of-Plane Drift Capacity of Stone Masonry Walls. *Buildings* **2023**, *13*, 437. [[CrossRef](#)]
37. García-Alba, J.; Bárcena, J.F.; García, A. Zonation of Positively Buoyant Jets Interacting with the Water-Free Surface Quantified by Physical and Numerical Modelling. *Water* **2020**, *12*, 1324. [[CrossRef](#)]
38. Bouarroudj, M.A.; Boudaoud, Z. Numerical Investigation of Predicting the In-Plane Behavior of Infilled Frame with Single Diagonal Strut Models. *Struct. Eng. Mech.* **2022**, *81*, 131–146. [[CrossRef](#)]

Disclaimer/Publisher's Note: The statements, opinions and data contained in all publications are solely those of the individual author(s) and contributor(s) and not of MDPI and/or the editor(s). MDPI and/or the editor(s) disclaim responsibility for any injury to people or property resulting from any ideas, methods, instructions or products referred to in the content.